The putative lytic transglycosylase VirB1 from *Brucella suis* interacts with the type IV secretion system core components VirB8, VirB9 and VirB11

Christoph Höppner,[1] Anna Carle,[1] Durga Sivanesan,[2] Sabine Hoeppner[3] and Christian Baron[1,2]

Correspondence
Christian Baron
baronc@mcmaster.ca

[1]Ludwig-Maximilians-Universität, Department Biologie I, Bereich Mikrobiologie, Maria-Ward-Str. 1a, D-80638 München, Germany

[2]McMaster University, Department of Biology, 1280 Main St West, Hamilton, ON, Canada LS8 4K1

[3]Ludwig-Maximilians-Universität, Gene Center, Feodor-Lynen Str. 25, D-81377 München, Germany

VirB1-like proteins are believed to act as lytic transglycosylases, which facilitate the assembly of type IV secretion systems via localized lysis of the peptidoglycan. This paper presents the biochemical analysis of interactions of purified *Brucella suis* VirB1 with core components of the type IV secretion system. Genes encoding VirB1, VirB8, VirB9, VirB10 and VirB11 were cloned into expression vectors; the affinity-tagged proteins were purified from *Escherichia coli*, and analyses by gel filtration chromatography showed that they form monomers or homo-multimers. Analysis of protein–protein interactions by affinity precipitation revealed that VirB1 bound to VirB9 and VirB11. The results of bicistron expression experiments followed by gel filtration further supported the VirB1–VirB9 interaction. Peptide array mapping identified regions of VirB1 that interact with VirB8, VirB9 and VirB11 and underscored the importance of the C-terminus, especially for the VirB1–VirB9 interaction. The binding sites were localized on a structure model of VirB1, suggesting that different portions of VirB1 may interact with other VirB proteins during assembly of the type IV secretion machinery.

INTRODUCTION

Type IV secretion systems (T4SS) are used by many Gram-negative bacteria to translocate virulence factors into eukaryotic cells or to mediate conjugative transfer of broad-host-range plasmids (Cascales & Christie, 2003; Celli & Gorvel, 2004; Llosa & O'Callaghan, 2004; Zupan *et al.*, 2000). T4SS are crucial determinants of host–pathogen interactions, which enable bacterial survival in widely different habitats, such as the rhizosphere of plants (*Agrobacterium tumefaciens*) and intracellular compartments of mammalian cells (*Brucella* species). The best-studied model is *A. tumefaciens*; its T4SS comprises 12 components, VirB1–VirB11 and VirD4. Biochemical, genetic and cell biological experiments suggest that VirB2–VirB11 constitute a membrane-spanning pore, which connects the inner and the outer membrane through periplasmic interactions and homo-oligomer formation, and an extracellular pilus (Cascales & Christie, 2003; Christie, 2004). VirD4 links this channel to translocated substrates (Atmakuri *et al.*, 2003; Kumar & Das, 2002). VirB6, VirB7, VirB8, VirB9 and VirB10 constitute the core of the T4SS and the substrate transfer route, although direct evidence for channel formation is still lacking. VirB2 and VirB5 are major and minor components of the extracellular pilus of *A. tumefaciens*, which probably mediates contact formation with the host cell (Eisenbrandt *et al.*, 1999; Hwang & Gelvin, 2004; Schmidt-Eisenlohr *et al.*, 1999). The role of the VirB3 protein is less well defined than those of other T4SS components, but its interaction with pilus components and localization in the outer membrane suggest that it may play a role during the assembly of this structure (Jones *et al.*, 1994; Shamaei-Tousi *et al.*, 2004; Yuan *et al.*, 2005). VirB4 and VirB11 are multimeric inner-membrane-localized NTPases, which may traverse the inner membrane to contact periplasmic VirB proteins (Atmakuri *et al.*, 2004; Dang & Christie, 1997; Middleton *et al.*, 2005; Yeo *et al.*, 2003; Yuan *et al.*, 2005). They may either act as assembly factors for the T4SS or drive pilus subunits or substrate molecules across the cell envelope. VirB2–VirB11 are indispensable both for gene transfer from *A. tumefaciens* and for *Brucella*'s ability to reach the proper intracellular niche and to replicate within HeLa cells or macrophages (Berger & Christie, 1994; Comerci *et al.*, 2001; O'Callaghan *et al.*, 1999; Sieira *et al.*, 2000).

Abbreviations: S2B, StrepII buffer; T4SS, type IV secretion system(s).

VirB1 is the only non-essential T4SS component. It was previously demonstrated that VirB1 homologues play an important role in the T4SS of *A. tumefaciens* and *Escherichia coli* strains harbouring plasmids pKM101 and R1. The efficiency of substrate transfer was reduced 10- to 1000-fold upon non-polar deletion of the encoding genes (Bayer *et al.*, 1995; Berger & Christie, 1994; Fullner, 1998; Winans & Walker, 1985). An infection assay with signature-tagged *Brucella abortus* mutants demonstrated that mutagenesis of the *virB1* gene causes attenuation of virulence (Hong *et al.*, 2000). A more recent study demonstrated that survival of *B. abortus* in macrophage cell cultures was attenuated in strains carrying a non-polar *virB1* mutation (den Hartigh *et al.*, 2004). Thus the deletion of genes encoding VirB1 homologues generally has an attenuating effect on T4SS-related functions. The *Helicobacter pylori* VirB1 homologue HP0523 is an exception to this rule, as it was shown to be essential for bacterial virulence (Odenbreit *et al.*, 2001; Rohde *et al.*, 2003). Due to the presence of highly conserved sequence motifs, VirB1 was identified as a putative lytic transglycosylase, but its specific role for T4SS function was not elucidated in detail. *A. tumefaciens* and *Brucella suis* VirB1 both possess a signal sequence and are therefore directed to the periplasmic space by the general secretion pathway (Llosa *et al.*, 2000; O'Callaghan *et al.*, 1999). Their enzymic activity probably leads to localized cell wall lysis, creating space for accommodation of the T4SS (Bayer *et al.*, 2001; Mushegian *et al.*, 1996; Zahrl *et al.*, 2005). Despite the well-known area of lysozyme biochemistry, proposals for the catalytic mechanism of lytic transglycosylases were published only recently. Whereas the well-known lysozymes like hen egg white lysozyme break up murein by hydrolysis of the $\beta(1\rightarrow4)$-glycosidic bond between the *N*-acetylmuramic acid (MurNAc)-C1 and the *N*-acetylglucosamine (GlcNAc)-C4, the lytic transglycosylases lyse this substrate in a transglycosylation reaction utilizing the C6-OH residue of the same MurNAc (Blackburn & Clarke, 2001; Koraimann, 2003). Thus, no water is required for the reaction, which produces a 1,6-anhydromuramic acid terminal residue. Special features of the active site that distinguish the lytic transglycosylases from lysozymes must explain the mechanistic difference, and this question is subject to structural biological studies (Lehnherr *et al.*, 1998; Leung *et al.*, 2001; Mushegian *et al.*, 1996; Thunnissen *et al.*, 1994; van Asselt *et al.*, 1999, 2000).

When VirB1 was identified as a lytic transglycosylase, its importance for the *A. tumefaciens* T4SS was largely attributed to its proposed catalytic activity. This notion was repeatedly confirmed by the observation that active-site mutants of the protein failed to fully complement *virB1* deletion strains (Höppner *et al.*, 2004; Mushegian *et al.*, 1996). After export across the inner membrane, VirB1 of *A. tumefaciens* is further processed in the periplasm, yielding a processing product of the C-terminal 73 amino acids designated VirB1* (Baron *et al.*, 1997). VirB1* and the N-terminus, representing the lytic transglycosylase domain, independently enhanced tumorigenicity, which implied an additional function of VirB1* (Llosa *et al.*, 2000). Further evidence for this hypothesis was generated when it was shown by co-immunoprecipitation that VirB9 interacts with VirB1* in *A. tumefaciens* (Baron *et al.*, 1997). A high-resolution dihybrid screen with protein components of the *A. tumefaciens* T4SS suggested self-interaction and a number of uni- and bidirectional interactions between VirB1 and VirB4, VirB8, VirB9, VirB10 and VirB11 (Ward *et al.*, 2002). Direct biochemical evidence for the interactions was not presented in that study.

In spite of the low overall amino acid sequence identity of 22 %, the VirB1 homologue from *B. suis* complemented *virB1* gene defects in *A. tumefaciens*, suggesting that it engages in similar interactions with T4SS components. Similarly, the *B. suis* VirB4 homologue complemented *virB4* gene defects in *A. tumefaciens* (Yuan *et al.*, 2005), which further supported the notion that the overall architecture of different T4SS is very similar (Christie, 2004; Yeo & Waksman, 2004). To directly test interactions of VirB1sp with T4SS core components we chose derivatives of VirB proteins from *B. suis*, (abbreviated VirBs in the following – or VirBsp to indicate periplasmic domains without signal peptides or membrane domains), which are more readily amenable to overproduction and purification than those from *A. tumefaciens*. Using different biochemical methods (affinity precipitation, gel filtration, bicistron expression, peptide array analysis), we showed that purified *B. suis* T4SS core components undergo different interactions. VirB1sp was found to interact with VirB9sp, and whereas this interaction was the strongest among those we investigated, VirB1sp also bound to VirB8sp and VirB11s. The binding sites were localized in a structure model of VirB1sp, suggesting that a sequence of transient interactions guides lytic transglycosylase function during T4SS assembly.

METHODS

Cultivation of bacteria. For overnight cultures all *E. coli* strains were grown in LB (1 % tryptone; 0·5 % yeast extract; 0·5 % NaCl) or LBON (1 % tryptone; 0·5 % yeast extract) under aerobic conditions at 37 °C in a laboratory shaker (modell Kühner, B. Braun) at 200 r.p.m. Carbenicillin (100 μg ml^{-1}) was included for selection of plasmid-carrying cells. Day cultures were inoculated to an OD_{600} of 0·05 in vessels of appropriate volume with the same media under vigorous shaking at 37 °C (Certomat-R, B. Braun Biotech International). The T7 promoter in the protein-overproducing strain GJ1158 (Bhandari & Gowrishankar, 1997) was induced at an OD_{600} of 0·4–0·8 by addition of 5 M NaCl stock solution to a final concentration of 0·3 M. Cultivation under aerobic conditions then proceeded at different temperatures for varying amounts of time for the overproduction of specific proteins as follows: VirB1s (C- or N-terminal tag) at 26 °C for 4 h, VirB1s/VirBsX (bicistron constructs) at 26 °C for 6 h, VirB7sp at 26 °C for 4 h, VirB8sp at 37 °C for 4 h, VirB9sp at 37 °C for 4 h, VirB10sp at 27 °C for 6 h, VirB11s at 27 °C for 18 h. The total culture volumes were 1 litre, in four 500 ml Erlenmeyer flasks each containing 250 ml LBON.

Molecular biology methods. Manipulations of DNA for plasmid isolation, PCR amplification, restriction, ligation and sequencing followed standard procedures, using enzymes from New England Biolabs and MBI Fermentas and *E. coli* JM109 as cloning host (Maniatis *et al.*, 1982; Yanisch-Perron *et al.*, 1985). PCR fragments

were first cloned into pCR2.1-TOPO (Invitrogen), followed by sequencing and further subcloning into expression vectors as described below.

Construction of *virB* gene expression vectors. Expression vectors for the production of VirBs proteins (Table 1) were constructed by PCR amplification of the genes with oligonucleotides, which introduced 5′ and 3′ restriction sites (sequences given in Table 2), followed by ligation into similarly cleaved vectors. Constructs for the overproduction of N-terminally tagged StrepIIVirB1sp and StrepII-VirB11s were generated by PCR amplification of the genes, cleavage with *Acc*65I/*Pst*I and *Acc*65I/*Hin*dIII, and ligation into similarly cleaved pT7-7StrepII (pT7-7StrepIIVirB8sp, pT7-7StrepIIVirB9sp and pT7-7StrepIIVirB10sp were described previously; Yuan *et al.*, 2005). The gene encoding VirB11s was subsequently subcloned using the same restriction sites into pT7-H_6TrxFus for expression as an N-terminally His_6TrxA-tagged fusion protein (pT7-H_6TrxVirB8sp, pT7-H_6TrxVirB9sp and pT7-H_6TrxVirB10sp were described previously; Yuan *et al.*, 2005). Similar procedures were applied for the cloning of VirB7s into pT7-H_6TrxFus using *Xba*I/*Pst*I restriction sites. pET24dVirB1spHis_6 for overproduction of C-terminally His_6-tagged VirB1sp was constructed by PCR cloning of the *virB1* gene and introduction of the *Nco*I/*Not*I-treated fragment into similarly cleaved pET24d.

Bicistron vectors for the co-expression of proteins and vectors for the production of untagged control proteins were constructed as follows. In order to co-produce C-terminally His_6-tagged VirB1sp with putative interaction partners, vector pET21BC was constructed by introducing a *Sal*I/*Not*I DNA fragment encoding *Schizosaccharomyces pombe* Srb11 including the ribosome-binding site (Baumli *et al.*, 2005). The first ORF of the pET21BC series encoded the putative interaction partner and was created by cleavage of the vector with *Nhe*I/*Eco*RI and insertion of PCR-amplified *virB8*, *virB9* and *virB10* genes treated with the same restriction endonucleases. After excision of the Srb11-encoding gene by cleaving the vector with *Nco*I/*Not*I, *virB1* was inserted using the same

Table 1. Plasmids

Plasmid	Genotype	Source or reference
pUC18VirB	$Carb^R$, *virB* region from *B. suis* 1330	O'Callaghan *et al.* (1999)
pCR2·1-TOPO	$Carb^R$ Kan^R, for direct cloning of PCR fragments	Invitrogen
pET24d	Kan^R, cloning and T7 expression vector	Novagen
pT7-7StrepII	$Carb^R$, for overexpression of N-terminally StrepII-tagged fusion proteins	Balsinger *et al.* (2004)
pT7-7StrepIIVirB8sp	pT7-7StrepII with 492 bp *Acc65*I/*Pst*I fragment of *virB8* from *B. suis*	Yuan *et al.* (2005)
pT7-7StrepIIVirB9sp	pT7-7StrepII with 813 bp *Acc65*I/*Pst*I fragment of *virB9* from *B. suis*	Yuan *et al.* (2005)
pT7-7StrepIIVirB10sp	pT7-7StrepII with 1020 bp *Acc65*I/*Pst*I fragment of *virB10* from *B. suis*	Yuan *et al.* (2005)
pT77-StrepIIVirB11s	pT7-7StrepII with 1083 bp *Acc65*I/*Hin*dIII fragment of *virB11* from *B. suis*	This work
pT7-H_6TrxFus	$Carb^R$, for T7-based expression of N-terminal His_6-TrxA (thioredoxin) fusions	Kromayer *et al.* (1996)
pT7-H_6TrxVirB7sp	pT7-H_6TrxFus with 126 bp *Xba*I/*Pst*I fragment of *B. suis virB7*	This work
pT7-H_6TrxVirB8sp	pT7-H_6TrxFus with 492 bp *Acc65*I/*Pst*I fragment of *B. suis virB8*	Yuan *et al.* (2005)
pT7-H_6TrxVirB9sp	pT7-H_6TrxFus with 813 bp *Acc65*I/*Pst*I fragment of *B. suis virB9*	Yuan *et al.* (2005)
pT7-H_6TrxVirB10sp	pT7-H_6TrxFus with 1020 bp *Acc65*I/*Pst*I fragment of *B. suis virB10*	Yuan *et al.* (2005)
pT7-H_6TrxVirB11s	pT7-H_6TrxFus with 1083 bp *Acc65*I/*Hin*dIII fragment of *VirB11* from *B. suis*	This work
pT7-7StrepIIVirB1sp	pT7-StrepII with 654 bp *Acc65*I/*Pst*I fragment of *virB1* from *B. suis*	This work
pET21BC	$Carb^R$, pET21b derivative with a DNA fragment encoding the *S. pombe* ribosome-binding site and SRB11 cloned with *Sal*I/*Not*I into pET21b (with two RBS in the polylinker) for T7-driven bicistronic expression; determines His_6-tagged C-terminus of second ORF	This work
pET24dVirB1spHis_6	Kan^R, pET24d with 654 bp *Nco*I/*Not*I *B. suis virB1* fragment	This work
pET21BCVirB8sp-VirB1spHis_6	pET21BC with 524 bp *Nhe*I/*Eco*RI *virB8* and 654 bp *Nco*I/*Not*I *B. suis virB1* fragment downstream	This work
pET21BCVirB9sp-VirB1spHis_6	pET21BC with 776 bp *virB9* and 654 bp *B. suis virB1* fragment downstream	This work
pET21BCVirB10sp-VirB1spHis_6	pET21BC with 1011 bp *virB10* and 654 bp *B. suis virB1* fragment downstream	This work
pET21BCVirB8sp	pET21BCVirB8sp-VirB1spHis_6, *virB1* gene removed with *Sal*I/*Xho*I and religated	This work
pET21BCVirB9sp	pET21BCVirB9sp-VirB1spHis_6, *virB1* gene removed with *Sal*I/*Xho*I and religated	This work
pET21BCVirB10sp	pET21BCVirB10sp-VirB1spHis_6, *virB1* gene removed with *Sal*I/*Xho*I and religated	This work

Table 2. PCR primers

Primer	Sequence*	Vector cloned in
VirB1s-5′	5′-CGATGGTACCCGCAATCGTGCAGGTCGAGTCGG-3′	pT7-7StrepII
VirB1s-3′	5′-CGATCTGCAGTTAGAAAACAACTACGCCGTCCG-3′	
VirB7s-5′	5′-GGGCCTCTAGAGTGCACTACAACGGGGCCG-3′	pT7-H_6TrxFus
VirB7s-3′	5′-CCGGCTGCAGTTAGTCCTCGTAAGTGTCAACGG-3′	
VirB11s-5′	5′-GCGCGGTACCCATGATGTCCAACCGAAGTGAC-3′	pT7-7StrepII and pT7-H_6TrxFus
VirB11s-3′	5′-CGTCAGAAGCTTATAAATTTGTGCAGCATATGCGT-3′	
Srb11-5′	5′-GGGGGGGTCGACAATAATTTTGTTTAACTTTAAG*AAGGAG*ATATA-CCATGGGTATGGCAGCAAATTACTGGGCCTCTAG-3′	pET21b
Srb11-3′	5′-GGGCCCGGGGCGGCCGCTTCAATATCCTCAAAATAATAAATAG-3′	
VirB1sBC5′:	5′-GCGCGCCCATGGCAGCAATCGTGCAGGTCGAGT-3′	pET21BC/pET24d
VirB1sBC3′:	5′-GACTGCGGCCGCGAAAACAACTACGCCGTCCG-3′	
VirB8sBC5′:	5′-GCGCGCTAGCCGCGTCAACGCACAGAC-3′	pET21BC
VirB8sBC3′:	5′-GCGCGAATTCTCATTGCACCACTCCCATTTCTGG-3′	
VirB9sBC5′:	5′-GCGCGCTAGCATTCAGTATGTCGATTACAATTC-3′	pET21BC
VirB9sBC3′:	5′-GCGCGAATTCTCATTGCAGGTTCTCCCCGGGC-3′	
VirB10sBC5′:	5′-GCGCGCTAGCGGCAATGCAGAGAATAATCACC-3′	pET21BC
VirB10sBC3′:	5′-GCGCGAATTCTCATTGCAGGTTCTCCCCGGGC-3′	

*Restriction sites are underlined and Shine–Dalgarno motifs are in *italics*.

restriction sites. This placed *virB1* in-frame with the vector sequence encoding the C-terminal His_6-tag. A series of constructs for the expression of non-tagged proteins was generated to serve as controls, as these proteins did not bind avidly to affinity columns. Based on the pET21BC bicistron vectors, three constructs that served as negative controls were created by excision of *virB1* with *Sal*I/*Xho*I and religation of the vector. Untagged VirB8sp, VirB9sp or VirB10sp were produced upon induction of expression from these vectors.

Strep-Tactin Sepharose chromatography. Bacterial cells were resuspended in 4–8 ml StrepII buffer (S2B) without DTT (300 mM NaCl, 100 mM Tris/HCl, 1 mM EDTA, pH 7·0) and with 0·5 mM PMSF and passed three times through a French pressure cell (Aminco) at 18 000 p.s.i. The lysate was centrifuged (SS34 rotor, 25 min, 13 000 r.p.m. at 4 °C) to remove cell debris and unbroken cells, and the N-terminal StrepII-fusion protein was purified with a 1 ml Strep-Tactin Superflow column following the instructions of the manufacturer (IBA), using 2·5 mM desthiobiotin in the elution buffer. The fractions were subsequently purified by size-exclusion chromatography using S2B at a flow rate of 0·5 ml min^{-1}. Superdex 75 or Superdex 200 (Amersham Pharmacia Biosciences) was used depending on the molecular mass of the protein. The samples were dialysed for >12 h against 1 litre of PSB (S2B with 50 % glycerol) in dialysis tubing (Visking, Roth) at 4 °C and were stored at −20 °C until further use. Protein concentrations were determined using the Bradford dye binding assay (Bio-Rad) with bovine serum albumin as a reference.

Immobilized metal chelate affinity chromatography (IMAC). Cells were lysed in S2B without DTT (0·5 mM PMSF) and centrifuged as described above; the supernatant was applied to an HPLC system (Äkta Purifier, Amersham Pharmacia Biotech) with a 5 ml Co^{2+}-charged IMAC column (Talon Superflow, Clontech). His_6-tagged recombinant protein was eluted according to a step-gradient protocol. At a flow rate of 0·5–1·0 ml min^{-1} the column was first washed for 5 column volumes. Then, a stringent washing step with 20 mM imidazole proceeded for 2·5 column volumes, before 150 mM imidazole was applied to the column for 2·5 column volumes. Both the stringent wash fractions and the elution fractions were collected in 2 ml aliquots, followed by gel filtration, dialysis in PSB and determination of the protein concentrations as described above.

Strep-Tactin Sepharose pull-down assay. Samples (10 µl) of purified StrepII-tagged proteins (5 pmol μl^{-1} in PSB) were incubated with 20 µl Strep-Tactin Sepharose (50 % suspension in S2B, IBA) for 15 min. Then 80 µl S2B and 10 µl His_6TrxA-fusion protein (5 pmol μl^{-1} in PSB) were added. After 15 min incubation at room temperature, the Sepharose matrix was sedimented (centrifugation at 13 000 r.p.m., 2 min) and washed three times with 500 µl S2B. Bound proteins were eluted with 35 µl 1 mM biotin followed by sedimentation of the matrix, mixing of the supernatant with 1 vol. Laemmli sample buffer, SDS-PAGE, Western blotting and analysis with VirB protein-specific antisera.

Gel filtration chromatography. Samples generated by affinity chromatography (1 ml maximum) were loaded onto Superdex 200 or Superdex 75 gel filtration columns in S2B; the flow rate was 0·5 ml min^{-1} or 1·0 ml min^{-1}. To determine the molecular mass of proteins, the columns were calibrated with the Gel Filtration Calibration Kit (Amersham Pharmacia Biotech), which uses reference proteins in the range between 13·7 and 669 kDa.

SDS-PAGE and Western blotting. Proteins were separated in denaturing SDS gels using the Laemmli system (Laemmli, 1970) followed by transfer to PVDF membranes (Immobilon-P, Millipore) in a vertical blot device (Trans Blot Cell, Bio-Rad; blot buffer 192 mM glycine, 25 mM Tris, 20 % methanol) at 90 V for 1 h or 30 V for 16 h (Harlow & Lane, 1988). Proteins attached to peptide array membranes (see below) were transferred in a semi-dry blot device (Fast-Blot, Biometra) onto PVDF membranes following a specialized protocol, followed by regeneration of the membrane as suggested by the manufacturer (Jerini). Proteins were detected with goat anti-rabbit IgG-HRP (Bio-Rad), a chemiluminescence detection system (Lumi Light, Roche Diagnostics) and X-ray film (Harlow & Lane, 1988).

Peptide array experiments. The entire sequence of VirB1sp from *B. suis* (GenBank accession no. NP_699276) without the signal peptide was displayed on a cellulose membrane as seventy 13-mers, covalently bound at the C-terminus and with N-terminal acetylation, shifting three amino acid positions each time, beginning with peptide 1 (AAIVQVESGFNPY), peptide 2 (VQVESGFNPYAIG), etc., to peptide 70 (PPGKDNTDGVVVF). The protocol for 'Mapping of discontinuous epitopes' from the manual of the supplier (Jerini) was followed. The peptide array membrane, which features all possible linear epitopes of VirB1sp, was preincubated for 30 min in TBS-T (20 mM Tris/HCl; 137 mM NaCl; 0·1 % Tween-20; pH 8·0), transferred into blocking solution (Roche) for 1 h, washed again with TBS-T for 10 min and then incubated in blocking solution containing 1–5 μg ml^{-1} of different proteins (StrepIIVirB1sp, StrepIIVirB8sp, StrepIIVirB9sp or StrepIIVirB11s) for 12 h at 4 °C. Before transfer of the attached proteins onto PVDF membranes with a semi-dry blot device (see above), the peptide array membrane was washed three times in TBS-T for 10 s to remove non-specifically bound protein.

Generation of polyclonal antisera. Soluble StrepIIVirB11s and H_6TrxAVirB7 were purified by affinity chromatography as described above, whereas StrepIIVirB1sp was obtained from a preparation of inclusion bodies, separated by SDS-PAGE, excised from the gel and subjected to electroelution. Approximately 0·5 mg of each protein was lyophilized and used for immunization of rabbits (BioGenes) to generate specific antisera. The other antisera used in this study were described elsewhere (Yuan *et al.*, 2005).

Graphical data processing. To capture images of polyacrylamide gels and chemoluminogramms, they were digitized using a UMAX UTC-6400 scanner, followed by processing with Photoshop 6.0 (Adobe) and Canvas 7.0 (Deneba Systems).

Protein sequence analysis. The CLUSTAL W (version 1.82) algorithm for multiple sequence alignment (Higgins, 1994) (http://www.ebi.ac.uk/clustalw) or EMBOSS for alignment of two less conserved amino acid sequences (Needleman & Wunsch, 1970; Smith & Waterman, 1981) (http://www.ebi.ac.uk/emboss/align) were applied. Sequence information was processed with NORSp (Liu & Rost, 2003) (http://cubic.bioc.columbia.edu/services/NORSp) in order to discover long regions without regular secondary structure. Predictions of secondary structure were obtained with the PHD algorithm (Rost, 1996) (http://www.embl-heidelberg.de/predictprotein). To create a conservation plot of sequence alignment, the alignment data were transferred to the AMAS server (Livingstone & Barton, 1993) (http://barton.ebi.ac.uk/servers/amas_server.html) using standard default values. All structure images were generated with DINO 9.0 (http://cobra.mih.unibas.ch/dino/intro.php).

RESULTS

Purification and characterization of affinity-tagged *B. suis* VirBs proteins

To analyse interactions of VirB1s with *B. suis* VirBs proteins the region of *virB1* encoding the predicted periplasmic domain of the protein without signal peptide was PCR-amplified and cloned into pT7-7-StrepII for expression with an N-terminal StrepII peptide (StrepIIVirB1sp) or into pET24d for expression with a C-terminal His_6 tag (VirB1spHis$_6$). The gene encoding full-length VirB11s was PCR-amplified and cloned into pT7-7StrepII for expression with an N-terminal StrepII peptide (StrepIIVirB11s). Similar clones for expression of StrepIIVirB8sp, StrepII-VirB9sp and StrepIIVirB10sp were described previously (Yuan *et al.*, 2005). The proteins were overproduced and purified via affinity columns, followed by gel filtration over a Superdex 200 column for further purification and analysis of their molecular masses. Analysis with a specific antiserum showed that both N- and C-terminally tagged variants of VirB1sp eluted in a broad molecular mass range; we have indicated the predicted sizes of monomers, dimers, tetramers and hexamers in Fig. 1. The relative distribution between the different forms varied between experiments and the hexameric form was not always prominent, suggesting a dynamic equilibrium between different multimeric forms. In addition, large portions of VirB1sp (70–80 %) eluted in the void volume in high-molecular-mass complexes (Fig. 1). The elution of lytic transglycosylases in high-molecular-mass complexes has also been observed by others and was shown to be due to binding of the proteins by GroEL (Zahrl *et al.*, 2005). The possibility that GroEL binds to VirB1sp was therefore assessed by Western blot analysis of the samples eluted from the gel filtration column using specific antisera, and we indeed detected co-elution of VirB1sp variants with GroEL in the void volume (not shown). Analysis of the molecular masses of the other VirBs proteins by gel filtration showed that they eluted as apparent monomers (StrepII-VirB8sp and StrepIIVirB9sp), dimers (StrepIIVirB10sp) or hexamers (StrepIIVirB11s) (Table 3). Varying degrees of high-molecular-mass aggregates eluting in the void volume of gel filtration columns were observed in all cases. The amounts varied in different overexpression experiments and could not be reduced by the addition of DTT or increased NaCl concentrations (not shown). Whereas we cannot exclude that these aggregates are of physiological relevance,

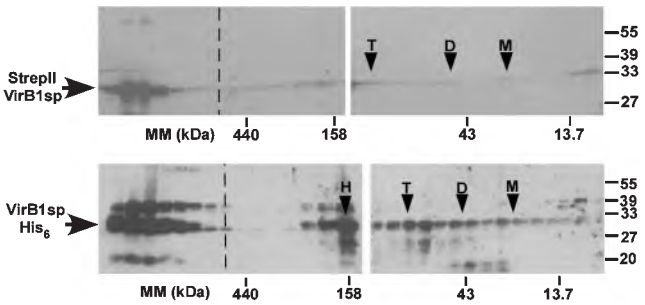

Fig. 1. Analysis of multimer formation of StrepIIVirB1sp and VirB1spHis$_6$ by gel filtration: Superdex 200 gel filtration analysis of the molecular masses of tagged VirB1sp variants after overproduction and purification by affinity chromatography. After gel filtration, the proteins in the eluted 2 ml fractions were separated by SDS-PAGE followed by Western blotting and detection with VirB1sp-specific antiserum. A dashed line marks the Superdex 200 void volume at >600 kDa. Arrowheads point to the expected sizes of monomeric (M), dimeric (D) tetrameric (T) and hexameric (H) proteins. Molecular masses of SDS-PAGE marker proteins are given on the right in kDa; the elution of gel filtration reference proteins with their associated molecular masses (MM) from the Superdex 200 column is indicated below the chemoluminograms.

Table 3. Molecular masses of StrepIIVirB proteins

Protein analysed	Expected mass of the monomer (kDa)	Mass determined by gel filtration (kDa)	Tertiary structure determined by gel filtration
StrepIIVirB1sp and VirB1spHis$_6$	27	Various to 160	Monomer, dimer, tetramer, hexamer
StrepIIVirB8sp	22	26	Monomer
StrepIIVirB9sp	33	41	Monomer
StrepIIVirB10sp	43	92	Dimer
StrepIIVirB11s	41	242	Hexamer

we did not consider this as very likely and used only the lower-molecular-mass fractions for the following studies.

Analysis of interactions by gel filtration

As a first approach to assess interactions between purified StrepIIVirBs proteins, mixtures of these proteins were co-incubated to allow complex formation. The samples were then subjected to gel filtration chromatography over a Superdex-200 column. Complex formation was assumed to lead to shifts of the elution volumes, but we did not observe changes in any case. This suggested that these proteins do not interact, or that the affinities are not high enough to form complexes stable during gel filtration (not shown).

We subsequently followed an alternative strategy based on the observation that recombinant proteins produced in *E. coli* are often insoluble or misfolded, and one reason for this is that their natural binding partners are absent. One method to circumvent this problem is the co-expression of the genes encoding such proteins together with genes encoding potential interaction partners (Lutzmann *et al.*, 2002). To this end, the potential interactions of VirB1sp with other components of the *B. suis* T4SS were tested by expression from vectors encoding C-terminally tagged VirB1spHis$_6$ fusion proteins and their putative interaction partners VirB8sp, VirB9sp or VirB10sp. In order to co-produce His$_6$-tagged VirB1sp with putative interaction partners, vector pET21BC was constructed to permit expression of bicistronic mRNAs. The first ORF of the pET21BC series encoded the putative interaction partners VirB8sp, VirB9sp and VirB10sp, and the second one VirB1spHis$_6$. In addition, a series of pET21BC-derived monocistronic constructs for the expression of the non-tagged interaction partners VirB8sp, VirB9sp or VirB10sp without VirB1spHis$_6$ was generated to serve as controls.

The proteins encoded on the pET21BC-derived vectors were overproduced in *E. coli*, followed by cell lysis, purification over a His$_6$-tag-specific affinity column and Superdex 200 gel filtration for analysis of complex formation. In spite of the two-step separation procedure, the untagged VirBsp proteins from both monocistronic and bicistronic expression experiments were detected in the gel filtration eluates, indicating that VirB8sp, VirB9sp and VirB10sp had non-specific binding affinity to the column. In order to distinguish between co-elution due to similar molecular masses and co-elution as an effect of an interaction, we compared the elution after expression from a bicistronic expression vector with that after expression from a monocistronic vector. VirB8sp eluted as a monomer in fractions 24–28 from the gel filtration in both cases, and VirB1spHis$_6$ eluted in fractions 17–21, supposedly the tetrameric and dimeric form (Fig. 2a). The co-expression with *virB8* thus had no apparent effect on the elution of VirB1spHis$_6$ and vice versa, suggesting that these two proteins did not interact. When VirB1spHis$_6$ was produced from the bicistronic vector with VirB10sp it eluted in fractions 17–19, which corresponded to the molecular mass expected for the tetramer (Fig. 2c). VirB10sp produced in strains carrying the monocistronic as well as the bicistronic vector eluted in fractions 17–19 as a dimer. As the molecular masses of VirB1spHis$_6$ and VirB10sp were very similar, this experiment did not give any evidence for an interaction. In contrast, when VirB1spHis$_6$ was produced from the bicistronic vector with VirB9sp it eluted from the column in three forms (Fig. 2b). First, it was detected in fractions 6–9, representing a large complex that had a lower molecular mass than that of VirB1spHis$_6$ when it was expressed from a monocistronic vector. Second, it eluted in fractions 15–17, corresponding to a complex markedly larger than the hexamer of 160 kDa, and third, it was detected in fractions 21–23, corresponding to a size between the dimer and tetramer. VirB9sp eluted in fractions 6–9 and 15–17 but the largest portion of the protein was monomeric (fractions 22–25). In contrast, when VirB9sp was expressed from the monocistronic vector, it predominantly eluted in fractions 22–25, which corresponded to the supposed monomer. It is evident from the comparison of the elution profiles that the co-expression with VirB9sp affected the oligomeric state of VirB1spHis$_6$ and vice versa. Whereas this method did not permit the unambiguous identification of hetero-oligomer formation, the results support a direct interaction between the two proteins. Alternative methods were employed in the following to further assess this possibility.

Analysis of interactions by affinity precipitation

An alternative way to demonstrate protein–protein interactions is a pull-down assay that exploits the affinity of the

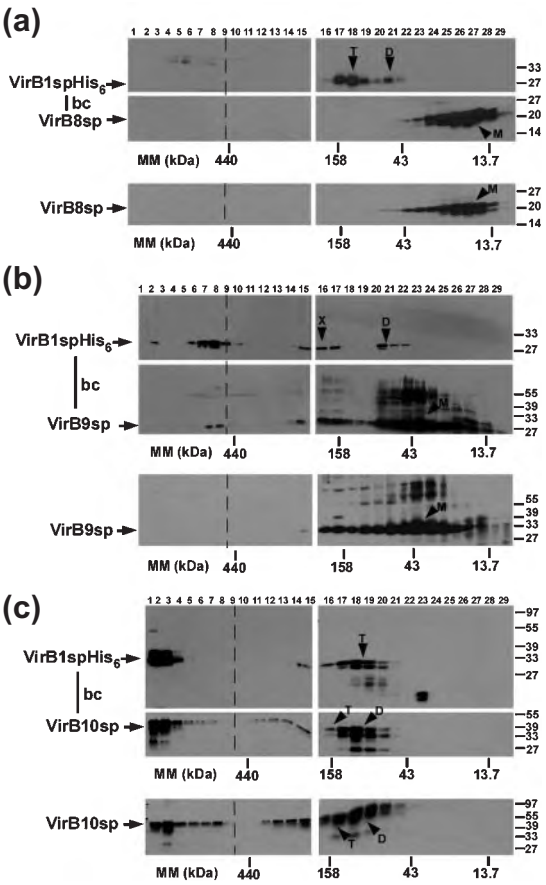

Fig. 2. Coelution of VirB1spHis$_6$ with other T4SS components: Superdex 200 gel filtration analysis of the molecular masses of VirB8sp (a), VirB9sp (b) and VirB10sp (c) expressed alone or from bicistronic vectors (bc) together with VirB1spHis$_6$ after overproduction and purification by affinity chromatography. After gel filtration, the proteins in the eluted 2 ml fractions were separated by SDS-PAGE followed by Western blotting and detection with specific antisera. Upper panels were probed with VirB1sp-specific antiserum, whereas lower panels were probed with antisera specific for VirB8sp (a), VirB9sp (b) and VirB10sp (c), respectively, as indicated by arrows. A dashed line marks the Superdex 200 void volume at $>$600 kDa. Arrowheads point to the expected size of monomeric (M), dimeric (D) and tetrameric (T) proteins. VirB1spHis$_6$ was detected in a complex of typical molecular mass (X), which was larger than the hexamer, exclusively after co-expression with VirB9sp. Molecular masses of SDS-PAGE marker proteins are given on the right in kDa; the elution of gel filtration reference proteins with their associated molecular masses (MM) from the Superdex 200 column is indicated below the chemoluminograms. All experiments were performed up to three times with similar results and the results of one set of representative experiments is shown.

StrepII tag for the Strep-Tactin Sepharose affinity matrix. The VirBs proteins that were tested for their capacity to bind StrepIIVirB1sp were affinity-purified as His$_6$-tagged thioredoxin fusions (His$_6$TrxA) and their co-precipitation with StrepII-tagged VirB1sp bound to the affinity matrix was determined. His$_6$TrxAVirB7sp, which was not expected to interact with VirB1sp, was included as a negative control for non-specific binding of the His$_6$TrxA affinity tag. Equimolar mixtures of StrepIIVirB1sp were incubated with His$_6$TrxA-VirB7sp, His$_6$TrxAVirB8sp, His$_6$TrxAVirB9sp, His$_6$TrxA-VirB10sp or His$_6$TrxAVirB11s, followed by sedimentation of the affinity matrix, washing and elution of StrepIIVirB1sp and attached binding partners with biotin, SDS-PAGE and Western blot analysis. His$_6$TrxAVirB7sp and His$_6$TrxA-VirB10sp did not co-precipitate with StrepIIVirB1sp, showing that these proteins did not interact under these conditions (Fig. 3). These results also demonstrated that the His$_6$TrxA tag had no affinity for the matrix utilized here. A different observation was made in the case of His$_6$TrxA-VirB8sp, which bound to the matrix irrespective of the presence of StrepIIVirB1sp. Since even extensive washing could not remove the protein from the Strep-Tactin matrix, it was impossible to use this method to assess this interaction. Co-fractionation with StrepIIVirB1sp was demonstrated in the case of His$_6$TrxAVirB9sp and His$_6$TrxA-VirB11s (Fig. 3). These results substantiate the interaction of VirB1sp with VirB9sp observed above and suggest that VirB11s may be another interaction partner. Since our experiments gave evidence for interactions of VirB1sp with VirB9sp and VirB11s, and VirB8sp may also interact with VirB1sp (Ward *et al.*, 2002), we next analysed the binding site(s) on VirB1sp using peptide array experiments.

Peptide array analysis of VirB1sp interactions

The analysis of binding to peptide arrays constitutes a high-resolution method to narrow down interaction site(s) on a protein, which has been used successfully for antibody epitope mapping and for the analysis of protein–protein interaction sites (Burns-Hamuro *et al.*, 2003; Knoblauch *et al.*, 1999; Llanos *et al.*, 1999; Reimer *et al.*, 2002; Reineke *et al.*, 1999). The analysis of multiple binding partners of different binding affinities in parallel permits a direct comparison of the bound region(s) and enables positive and negative control experiments. To this end, the binding of StrepIIVirB8sp, StrepIIVirB9sp and StrepIIVirB11s to 70 peptides displayed on membranes (13 amino acids long, three amino acids overlap), which represented the entire sequence of the processed form of VirB1sp, was analysed. Three identical membranes were used in parallel experiments, and they retained StrepIIVirBs proteins in every case. Western blots from five independent experiments, which determined the binding of an interaction partner to specific peptides, were graphically superimposed to obtain a representative mean result (Fig. 4a–c). The intensity of the signal for each spot was categorized from 1 (weak) to 4 (very strong). By aligning the sequences of the bound peptides, which overlapped by three amino acids, it was possible to identify domains of VirB1 that bind the respective VirBsp protein (Fig. 4d). When more than one spot defined an interacting domain in the sequence, the highest value of signal intensity present was assigned to the entire domain.

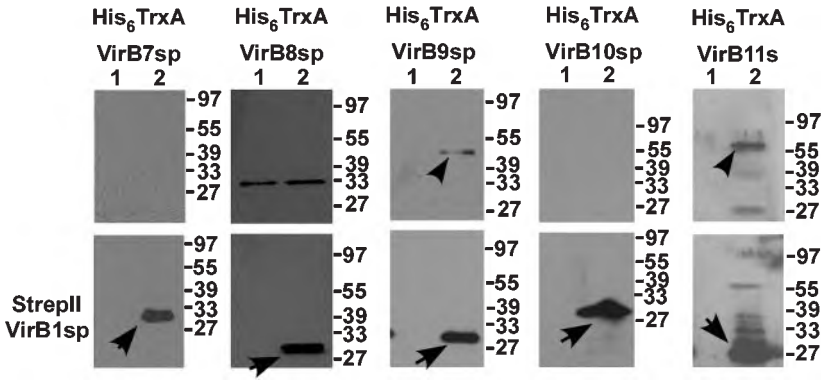

Fig. 3. Strep-Tactin Sepharose pull-down assay with StrepIIVirB1sp. StrepIIVirB1sp was preincubated with the Strep-Tactin matrix before addition of the indicated His_6TrxAVirBsp proteins. After washing three times, proteins were eluted from the matrix with 1 mM biotin, and analysed by SDS-PAGE, Western blotting and detection with specific antisera. Lower panels were probed with VirB1sp-specific antiserum, whereas upper panels were probed with antisera specific for VirB7sp, VirB8sp, VirB9sp, VirB10sp and VirB11s, respectively. Lanes 1 show the negative controls of only His_6TrxAVirBsp proteins incubated with the matrix; lanes 2 show the pull-down assays after co-incubation with StrepIIVirB1sp. Arrows indicate StrepIIVirB1sp sedimented with the matrix; arrowheads indicate co-sedimenting interaction partners. Experiments were repeated five times and representative results are shown. Molecular masses of reference proteins are shown on the right in kDa.

The three studied proteins StrepIIVirB8sp, StrepIIVirB9sp and StrepIIVirB11s bound to peptides from different regions of VirB1sp and the binding strengths were different, as indicated by the numbers of bound peptides and the signal intensity on the chemoluminogram. StrepIIVirB9sp bound to the highest number of VirB1sp peptides, but StrepIIVirB8sp and StrepIIVirB11s also bound to a defined set of VirB1sp peptides. To place this information in the context of the protein structure, a prediction of the VirB1sp secondary structure was done with the PHD algorithm and the proposed secondary structure is also shown in Fig. 4(a–c). Weak binding of StrepIIVirB8sp occurred to a region C-terminal to the catalytic Glu^{27} residue, which is predicted to be a loop/β-sheet region (Fig. 4a). StrepIIVirB8sp strongly interacted with another loop region N-terminal to the C-terminus. StrepIIVirB9sp bound to different amino acid stretches throughout the entire sequence of VirB1 (Fig. 4b). Interactions of intermediate strength occurred with three parts of the VirB1sp sequence that are only three amino acids long. StrepIIVirB9sp bound to the first three amino acids following the predicted signal peptide of VirB1, a loop region C-terminal to a short β-sheet and N-terminal to the conserved GIAQ motif, which is characteristic of all soluble lytic transglycosylases. An extended domain bound with intermediate strength by StrepIIVirB9sp was localized to the C-terminus of VirB1. Strong interactions with the amino acids C^{127}-Y^{128}-Y^{129} were observed, which are predicted to participate in the formation of an α-helix N-terminal to the C-terminus. Very strong binding to a loop region shortly after the GIAQ motif and N-terminal to the start of the C-terminus was detected. In addition, two long amino acid sequence stretches in the C-terminus were strongly recognized by StrepIIVirB9sp (Fig. 4b). StrepIIVirB11s bound only to a limited set of peptides on the VirB1sp array membrane (Fig. 4c). A weak interaction of StrepIIVirB11s with the VirB1sp sequence was apparent in a loop/β-sheet region C-terminal to the catalytic Glu^{27}. Strong binding to an α-helix/loop region and to a loop region in the amino acid sequence constituting the second half of the lytic transglycosylase domain was detected. A very strong interaction of StrepIIVirB11s was observed with a short loop region C-terminal to the GIAQ motif. These results further substantiated the interactions of VirB1sp with other T4SS components shown by different methods above. Interacting amino acids are often found in external loop regions, but a structure of VirB1sp was not available. To further assess the biological relevance of these interactions it was necessary to place the information on bound peptides in the context of a three-dimensional structure, and a model of the VirB1sp structure was generated next.

Modelling of the VirB1 structure and localization of its VirB protein interaction site(s)

To assess whether the sequence stretches of VirB1sp that interact with other proteins are spatially clustered and are conserved among different VirB1-like proteins, the X-ray structure of the soluble lytic transglycosylase Slt70 from *E. coli* was used as a model to approximate the structure of *B. suis* VirB1. To identify residues conserved among VirB1-like proteins, several of them were aligned with *E. coli* Slt70 (Fig. 5a). Next, the AMAS algorithm was used to assign values expressing the degree of conservation to all amino acid positions in a multiple sequence alignment, ranging from A (identical) to 8 (weakly conserved). One of the sequences in this alignment was a protein with known tertiary structure (here *E. coli* Slt70) and the other was *B. suis*

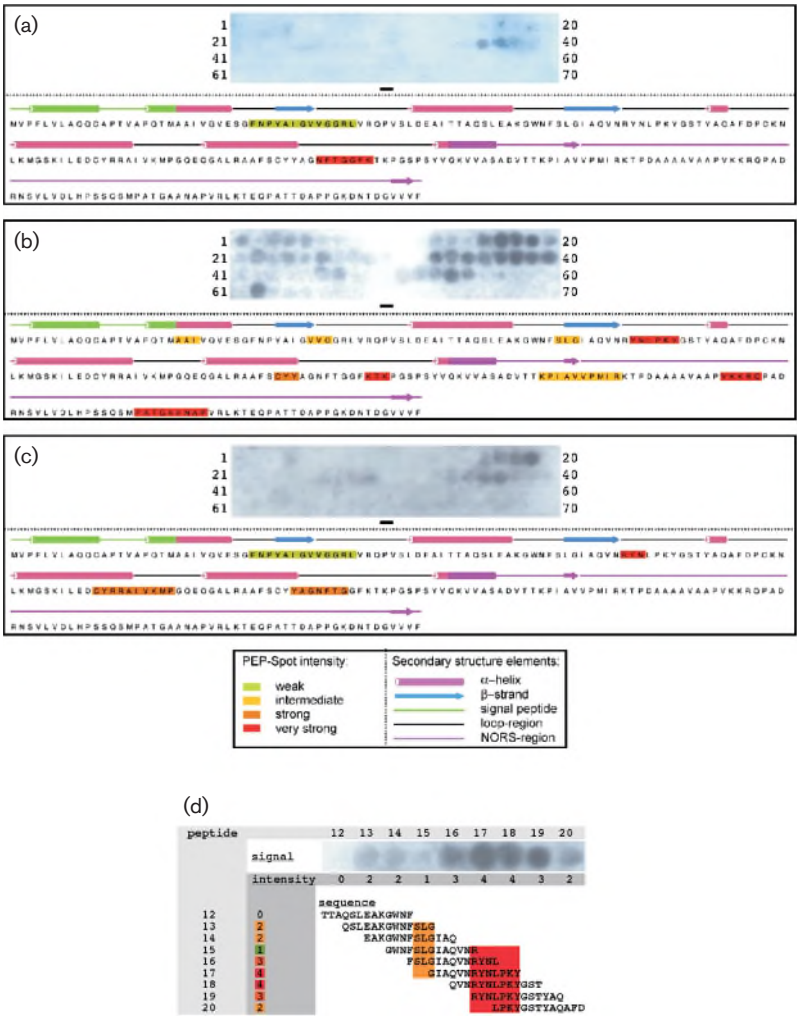

Fig. 4. Binding of StrepIIVirB8sp, StrepIIVirB9sp and StrepIIVirB11s to VirB1sp peptide array membranes. Binding of tagged VirB8sp (a), VirB9sp (b) and VirB11s (c) to VirB1sp peptides spotted on membranes (pepspot arrays) was determined by Western blot transfer of the bound proteins to PVDF membranes, followed by detection with specific antisera. The chemoluminograms represent the results of five independent experiments, which were graphically superimposed. A colour code is used to indicate the intensity of VirB protein binding (pepspot intensity) for every stretch of the corresponding VirB1 sequence. Secondary structure elements and the proposed signal peptide of VirB1 as predicted by the PHD algorithm (Rost, 1996) are also displayed below the chemoluminograms. (d) Method of peptide array evaluation. Signals from the Western blot (as an example for illustration, an enlarged portion from the VirB1sp membrane incubated with StrepIIVirB9sp is shown) were categorized by visual inspection, and the intensity values (1, weak, 2, intermediate, 3, strong, 4, very strong) assigned to a certain peptide number and colour. By alignment of the overlapping peptide, the sequence responsible for the observed signal (binding of StrepIIVirB9sp) can be identified. In the case of 'RYNLPKY', shown here, the most intense signal was categorized as 4 (very strong), and this value and the corresponding colour (red) were assigned to the entire sequence stretch.

VirB1. The software DINO was next applied to create a map of conserved residues on the surface of the known three-dimensional model (Fig. 5b, c). It is assumed that conserved patches on the surface are likely to interact either with partner proteins or substrate(s). Following the modelling we found that many of the amino acids conserved between VirB1 and Slt70 were not exposed on the surface but rather seem to stabilize the structurally conserved lysozyme fold. The most prominent conserved surface patch was the active-site cleft with the catalytic Glu residue, which is ubiquitously found throughout all lysozyme-like enzymes (Fig. 5b, c). The C-terminus of VirB1s did not align with Slt70 and it is thus not part of the model.

Next, the model was used to localize the interaction sites with StrepIIVirB8sp, StrepIIVirB9sp and StrepIIVirB11s on the surface of the VirB1sp model (Fig. 5d). The peptide array experiments yielded signals of different intensities corresponding to peptides featuring parts of the VirB1sp sequence. The corresponding sequences were aligned, and defined regions of interaction. For each interacting region, the intensity of the signals constituting it was categorized into four classes, from 'weak' to 'very strong'. This classification did not compare signal intensities between peptide array experiments with different proteins and therefore, a 'strong' interaction of VirB1sp peptides with StrepIIVirB8sp might be classified as 'intermediate' in a peptide array with StrepIIVirB9sp. The studies are therefore semi-quantitative and need to be followed up by more quantitative methods in future. StrepIIVirB8sp and StrepIIVirB9sp apparently interacted with surface-exposed loop regions of VirB1sp that are most probably situated on different sides of the protein, and StrepIIVirB11s may bind to a part of the protein that connects these two (Fig. 5d). Interestingly, both StrepIIVirB9sp and StrepIIVirB11s bound strongly to peptides representing a not well-conserved part of the protein C-terminal to the second region, which is probably required for enzymic activity (boxed in Fig. 5a). Similarly, both StrepIIVirB8sp and StrepIIVirB9s bound strongly C-terminal to the third region implicated in enzyme activity of lytic transglycosylases (boxed in Fig. 5a). Most of the proposed interactions between VirB1sp and StrepIIVirB9sp could not be visualized in this model since they map to the C-terminal region of VirB1sp, which lacks a counterpart in Slt70. Nevertheless, the identification of binding sites for other T4SS components in a structure

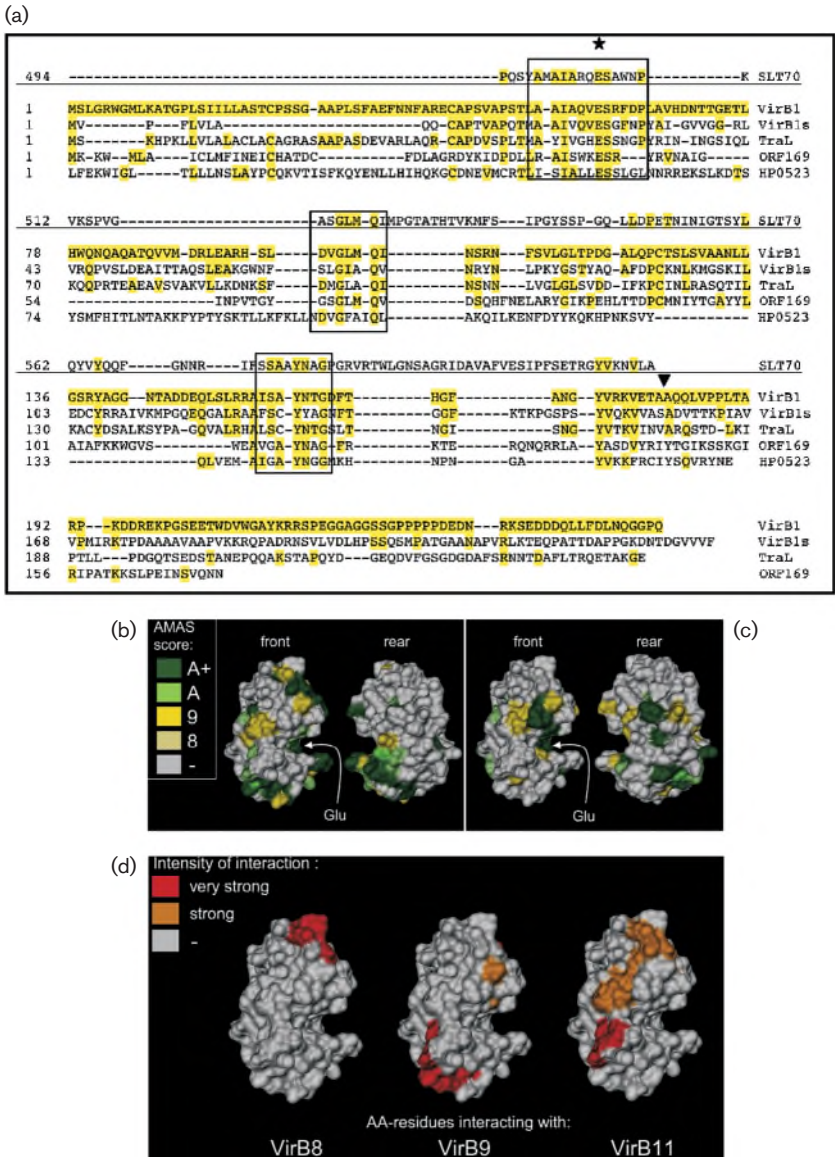

Fig. 5. Prediction of conserved surface residues in different lytic transglycosylases and regions of VirB1sp peptide arrays bound by StrepIIVirBs proteins. (a) Multiple sequence alignment of VirB1-like proteins. Residues identical to *A. tumefaciens* VirB1 are shaded; conserved residues implicated in the enzymic activity are indicated by black frames. The putative active-site Glu is labelled with a star; the cleavage site of *A. tumefaciens* VirB1 is indicated with a black arrowhead. The alignment of the VirB1 orthologues was generated with the MegAlign program, the SLT domain of *E. coli* Slt70 was aligned to *B. suis* VirB1 with EMBOSS (Needle algorithm) and fitted into the alignment. Amino acids conserved between the lytic transglycosylase domain of *B. suis* VirB1 and *E. coli* Slt70 (b) or *A. anser* LysG and *E. coli* Slt70 (c) are displayed on the surface of the Slt70 soluble lytic transglycosylase domain. The results from an EMBOSS alignment were processed and submitted to the AMAS server to validate the degrees of conservation. Identical residues in each of the two pairs are shown in dark green [A+], high similarity [A] in green, and lower similarity is in yellow [9] and light yellow [8]. The figure was prepared with DINO and the active-site Glu residue is indicated. (d) View of the Slt70 lytic transglycosylase domain surface structure taken as a model for VirB1sp. Interactions with StrepIIVirB8sp, StrepIIVirB9sp and StrepIIVirB11s as defined by the peptide array experiments are shown. A grey colour indicates no significant interaction; orange colour indicates strong and red colour very strong interaction.

model of VirB1sp constitutes a substantial advance in our understanding of the biological role of this protein. Our work lays the foundation for detailed structure–function analyses in future.

DISCUSSION

A role of VirB1 as nucleation centre for T4SS assembly has been suggested before, but hitherto, the interactions of VirB1 with T4SS components had only been demonstrated in the yeast dihybrid system (Ward *et al.*, 2002). Here we have directly studied the interaction of VirB1sp with most of its proposed interaction partners. This analysis was possible because the *B. suis* T4SS components are more amenable to biochemical experiments than their counterparts from the *A. tumefaciens* T4SS. Many of its components are relatively easy to purify, because in contrast to those from *A. tumefaciens*, they can be overexpressed in a soluble form with high yield, followed by affinity purification. This feature was exploited to conduct biochemical experiments to assess the suggested interactions. A portion of StrepIIVirB1sp and VirB1spHis$_6$ eluted from gel filtration columns in a multimeric protein complex (or aggregate) together with GroEL. We did not pursue the analysis of this complex further, as we did not consider it as the physiologically relevant form. Apart from that, VirB1spHis$_6$ was mainly present in the dimeric and tetrameric state and with reduced prominence as a hexamer. A larger portion of StrepIIVirB1sp was present in the high-molecular-mass complex, but it was also detected as lower-molecular-mass multimer. The available data suggest that StrepIIVirB1sp forms homomultimeric assemblies, probably dimers and tetramers. The molecular sieving effect of the murein layer prohibits diffusion of globular proteins or protein assemblies larger than 55 kDa (Höltje, 1998). Since the permeation of the

murein layer might be important for the function of lytic transglycosidase in the periplasm, the formation of dimers (approx. 50 kDa) appears to be more plausible in the natural biological context than the formation of tetramers (approx. 100 kDa), which may not permeate the murein layer.

The purified *B. suis* VirB proteins were then used to systematically assess the predicted interactions with VirB1sp. Some of those interactions were confirmed here, whereas others were only weak or not observed. Using co-elution and pull-down assays we did not get any evidence for an interaction between VirB1sp and VirB8sp or VirB10sp, which had been predicted from a previous yeast two-hybrid study (Ward *et al.*, 2002). In contrast, data from the peptide array experiment suggested that a set of VirB1sp peptides interacted with StrepIIVirB8sp, which supports the notion that these two proteins interact at least transiently. The evidence is not as substantial as that in case of StrepIIVirB9sp discussed below, suggesting that the interaction is weaker and/or may need additional interaction partners. These results are in line with the supposed role of VirB8 as nucleation factor, which undergoes transient interactions with many T4SS components (Kumar & Das, 2001; Yuan *et al.*, 2005). The *in vitro* data therefore argue against the postulated mechanism implying the VirB8–VirB1 interaction as key step for T4SS assembly (Ward *et al.*, 2002), but we can not rule out that the interaction is stronger *in vivo*.

Similar to VirB8sp, we obtained evidence for an interaction of the hexameric ATPase VirB11s with VirB1sp using peptide array as well as pull-down experiments. The interaction between VirB1sp and VirB9sp was demonstrated using a variety of different assays such as a pull-down assay and co-elution of the two proteins following their co-expression in a bicistronic construct. Peptide array experiments identified several StrepIIVirB9sp-interacting peptides throughout the VirB1sp sequence, and a considerable portion of them was in the C-terminus. Whereas this might argue for non-specific binding of StrepIIVirB9sp to the VirB1sp-derived peptides, we do not favour this interpretation for the following reasons. First, we have tested the binding of StrepII-VirB9sp to a pepspot membrane displaying the VirB5sp sequence, and, in line with other results showing that it does not bind strongly to VirB5sp, no non-specific binding to the membrane was observed (unpublished observations). Second, we observed non-specific binding of StrepIIVirB1sp as reflected by binding to most peptides on the VirB1sp pepspot membrane. Both the extent and strength of the signal were drastically elevated as compared to the relatively modest signal of bound StrepIIVirB9sp (unpublished observations). Finally, the peptide array data are very much consistent with the results of a previous study in intact cells, which demonstrated the interaction of the VirB1 C-terminus with VirB9 in *A. tumefaciens* (Baron *et al.*, 1997). We therefore conclude that the binding by StrepIIVirB9sp to many peptides of VirB1sp is likely to be of biological relevance.

The interaction with VirB9sp via the C-terminus is intriguing and this domain appears to play an important role for the functionality of the protein. Sequence analyses of a number of VirB1 homologues demonstrated special properties of the C-terminal part. The processed *A. tumefaciens* VirB1 C-terminus VirB1* (Baron *et al.*, 1997) and also the C-termini of *B. suis* VirB1 and pKM101 TraL were classified as NORS regions. These are regions of more than 70 amino acids in length that show less than 12 % secondary structure elements and an amino acid composition different from loop regions. It was demonstrated that these very flexible regions show similar degrees of conservation as other domains in similar proteins, and that they are more abundant in proteins with functions as regulators or transcription factors than in those with functions in biosynthesis or energy metabolism-related proteins (Liu & Rost, 2003). This implies important functional roles, most likely for transient protein–protein interactions with different partners. Only 4 % of all prokaryotic proteins contain NORS regions, and among the VirB proteins from *A. tumefaciens* and *B. suis*, channel component VirB10, which is supposedly involved in a high number of interactions (Cascales & Christie, 2003, 2004), is the only other protein that possesses such a region. Most interacting amino acid stretches identified here constitute loop or NORS regions, which are especially suited for establishing transient protein–protein interactions, suggesting that the interaction sites are biologically relevant.

To assess the biological relevance of the interactions and binding site(s) identified here, we pursued a modelling approach based on the known X-ray structure of a soluble lytic transglycosylase enzyme. To date, the structures of 18 murein-lytic lysozymes from different organisms have been solved. In addition, the three structures of the lytic transglycosylases LaL from bacteriophage λ, Slt35 and Slt70 (both from *E. coli*) are also available (Leung *et al.*, 2001; Thunnissen *et al.*, 1994; van Asselt *et al.*, 2000). The enzymic action of lysozymes and soluble lytic transglycosylases differs, but the protein fold is highly conserved (Mushegian *et al.*, 1996). Sequence comparison of *B. suis* VirB1 with two murolytic enzymes, whose X-ray structure was known, yielded intriguing results. The soluble lytic transglycosylase portion of Slt70 from *E. coli* ranges from amino acid P494 to A620 and has a significant degree of sequence similarity to *B. suis* VirB1 (identical, 23·1 %; similar, 38·1 %; gaps, 35·6 %). Other proteins like the lysozymes LysG from *Anser anser* (identical, 18·0 %; similar, 33·1 %; gaps, 23·8 %) and *Gallus gallus* LysC are less similar, although they were previously chosen to model the structure of *A. tumefaciens* VirB1 (Mushegian *et al.*, 1996). Structural superposition shows that despite an almost identical tertiary structure of LysG and Slt70 (Koraimann, 2003), their sequence similarity (identical, 22·0 %; similar, 36·3 %; gaps, 32·7 %) is less than that between Slt70 and VirB1. It was therefore appropriate to use the surface model of Slt70 to visualize regions of VirB1sp interaction with other VirB proteins. If the amino acids identified here by peptide array analysis were important for interactions they would be expected to localize on the surface of a protein. We indeed localized the

Table 4. Suggested and proven interactions of VirB1

The data for the predicted VirB protein localizations and interactions detected with dihybrid assays are from other publications as indicated and refer to the *A. tumefaciens* T4SS. IM, inner membrane; OM, outer membrane; ND, Not determined.

Protein	Localization (Cascales & Christie, 2003)	VirB1 interaction shown by:			
		Dihybrid analysis (Ward *et al.*, 2002)	Pull-down assay	Co-elution	Peptide array
VirB1	Periplasm	+	ND	+	ND
VirB8	IM	+	ND	−	+
VirB9	OM	+	+	+	+
VirB10	IM	+	−	−	ND
VirB11	IM	+	+	ND	+
VirB4	IM	+	ND	ND	ND

binding sites for StrepIIVirB8sp, StrepIIVirB9sp and StrepIIVirB11s on the surface of StrepIIVirB1sp, and these amino acids were not involved in the stabilization of the tertiary structure, which further substantiates the validity of the model. The model suggests that there was no apparent interference with the active-site cleft, but all three proteins bound C-terminally to residues likely to be involved in enzyme activity (regions 2 and 3 boxed in Fig. 5a). Thus, the binding may modulate enzyme activity; this possibility will be directly addressed in future.

Taken together, the results presented here suggest that VirB1s is a self-interacting protein that establishes transient contacts with other VirB proteins, such as VirB8s, VirB9s and VirB11s. A comparison of these results with predictions and results of previous studies is given in Table 4. A large amount of information on the role of VirB1-like proteins was collected in previous studies (Baron *et al.*, 1997; Höppner *et al.*, 2004; Llosa *et al.*, 2000; Mushegian *et al.*, 1996; Ward *et al.*, 2002; Zahrl *et al.*, 2005). Together with this analysis of protein interactions of VirB1s from the *B. suis* T4SS and the results from functional studies conducted with both the *A. tumefaciens* and *B. suis* T4SS, the following model was designed describing the function(s) of VirB1. Upon expression of the *virB* operon, all VirB proteins possessing an N-terminal signal peptide are exported into the periplasm or partially traverse the inner membrane. VirB1 may form a 50 kDa homodimer, which may render the active site inaccessible. The predicted pore size of the peptidoglycan layer permits diffusion of globular proteins smaller than 55 kDa, and therefore VirB9, VirB7, VirB5, VirB2 and the VirB1 dimer probably diffuse freely in the periplasm. The contact between VirB1 and VirB9 may be mediated by the C-terminus of VirB1 and lead to activation of the lytic transglycosylase activity of VirB9-bound VirB1. Transient interactions of VirB1 with VirB8 and VirB11 may facilitate this process, which may lead to a conformational change, followed by processing of VirB1 at its VirB1* cleavage site. The enzyme activity may be modulated by binding of VirB8, VirB9 or VirB11 close to active-site residues. Assembly of VirB7 and VirB9, which subsequently recruit other channel components such as VirB10 and VirB8, may accompany the opening of the cell wall. The N-terminal lytic transglycosylase domain of VirB1 (B1N) may subsequently be degraded in order to protect cellular integrity, whereas the C-terminal domain may remain attached to VirB9. VirB1* may exert an additional function in host cell recognition. As VirB1-like proteins can apparently be exchanged between different T4SS (Höppner *et al.*, 2004; Zahrl *et al.*, 2005), the results of these studies will probably be applicable to a wide variety of VirB1-like proteins from T4SS and other secretion systems (Koraimann, 2003).

ACKNOWLEDGEMENTS

We are indebted to August Böck (Munich, Germany) for continued support and Günter Koraimann (Graz, Austria) for discussions and the communication of results prior to publication. This work was supported by operating grants from the European Union Frame Programme 5 (contract QLK2-CT-2001-01200), by the Canadian Institutes of Health Research (CIHR grant MOP-64300) and by the Canada Foundation for Innovation (CFI) and the Ontario Innovation Trust (OIT) to C. Baron.

REFERENCES

Atmakuri, K., Ding, Z. & Christie, P. J. (2003). VirE2, a type IV secretion substrate, interacts with the VirD4 transfer protein at cell poles of *Agrobacterium tumefaciens*. *Mol Microbiol* **49**, 1699–1713.

Atmakuri, K., Cascales, E. & Christie, P. J. (2004). Energetic components VirD4, VirB11 and VirB4 mediate early DNA transfer reactions required for bacterial type IV secretion. *Mol Microbiol* **54**, 1199–1211.

Balsinger, S., Ragaz, C., Baron, C. & Narberhaus, F. (2004). Replicon-specific regulation of small heat shock genes in *Agrobacterium tumefaciens*. *J Bacteriol* **186**, 6824–6829.

Baron, C., Llosa, M., Zhou, S. & Zambryski, P. C. (1997). C-terminal processing and cellular localization of VirB1, a component of the T-complex transfer machinery of *Agrobacterium tumefaciens*. *J Bacteriol* **179**, 1203–1210.

Baumli, S., Hoeppner, S. & Cramer, P. (2005). A conserved mediator hinge revealed in the structure of the MED7·MED21 (Med7·Srb7) heterodimer. *J Biol Chem* **280**, 18171–18178.

Bayer, M., Eferl, R., Zellnig, G., Terferle, K., Dijkstra, A., Koraimann, G. & Högenauer, G. (1995). Gene *19* of plasmid R1 is required for both efficient conjugative DNA transfer and bacteriophage R17 infection. *J Bacteriol* **177**, 4279–4288.

Bayer, M., Iberer, R., Bischof, K., Rassi, E., Stabentheiner, E., Zellnig, G. & Koraimann, G. (2001). Functional and mutational analysis of P19, a DNA transfer protein with muramidase activity. *J Bacteriol* **183**, 3176–3183.

Berger, B. R. & Christie, P. J. (1994). Genetic complementation analysis of the *Agrobacterium tumefaciens virB* operon: *virB2* through *virB11* are essential virulence genes. *J Bacteriol* **176**, 3646–3660.

Bhandari, P. & Gowrishankar, J. (1997). An *Escherichia coli* host strain useful for efficient overproduction of cloned gene products with NaCl as the inducer. *J Bacteriol* **179**, 4403–4406.

Blackburn, N. T. & Clarke, A. J. (2001). Identification of four families of peptidoglycan lytic transglycosylases. *J Mol Evol* **52**, 78–84.

Burns-Hamuro, L. L., Ma, Y., Kammerer, S. & 7 other authors (2003). Designing isoform-specific peptide disruptors of protein kinase A localization. *Proc Natl Acad Sci U S A* **100**, 4072–4077.

Cascales, E. & Christie, P. J. (2003). The versatile bacterial type IV secretion systems. *Nat Rev Microbiol* **1**, 137–149.

Cascales, E. & Christie, P. J. (2004). *Agrobacterium* VirB10, an ATP energy sensor required for type IV secretion. *Proc Natl Acad Sci U S A* **101**, 17228–17233.

Celli, J. & Gorvel, J. P. (2004). Organelle robbery: *Brucella* interactions with the endoplasmic reticulum. *Curr Opin Microbiol* **7**, 93–97.

Christie, P. J. (2004). Type IV secretion: the *Agrobacterium* VirB/D4 and related conjugation systems. *Biochim Biophys Acta* **1694**, 219–234.

Comerci, D. J., Martinez-Lorenzo, M. J., Sieira, R., Gorvel, J. P. & Ugalde, R. A. (2001). Essential role of the VirB machinery in the maturation of the *Brucella abortus*-containing vacuole. *Cell Microbiol* **3**, 159–168.

Dang, T. A. & Christie, P. J. (1997). The VirB4 ATPase of *Agrobacterium tumefaciens* is a cytoplasmic membrane protein exposed at the periplasmic surface. *J Bacteriol* **179**, 453–462.

den Hartigh, A. B., Sun, Y. H., Sondervan, D., Heuvelmans, N., Reinders, M. O., Ficht, T. A. & Tsolis, R. M. (2004). Differential requirements for VirB1 and VirB2 during *Brucella abortus* infection. *Infect Immun* **72**, 5143–5149.

Eisenbrandt, R., Kalkum, M., Lai, E. M., Lurz, R., Kado, C. I. & Lanka, E. (1999). Conjugative pili of IncP plasmids, and the Ti plasmid T pilus are composed of cyclic subunits. *J Biol Chem* **274**, 22548–22555.

Fullner, K. J. (1998). Role of *Agrobacterium virB* genes in transfer of T complexes and RSF1010. *J Bacteriol* **180**, 430–434.

Harlow, E. & Lane, D. (1988). *Antibodies: a Laboratory Manual*. Cold Spring Harbor, NY: Cold Spring Harbor Laboratory.

Higgins, D. G. (1994). CLUSTAL V: multiple alignment of DNA and protein sequences. *Methods Mol Biol* **25**, 307–318.

Höltje, J. V. (1998). Growth of the stress-bearing and shape-maintaining murein sacculus of *Escherichia coli*. *Microbiol Mol Biol Rev* **62**, 181–203.

Hong, P. C., Tsolis, R. M. & Ficht, T. A. (2000). Identification of genes required for chronic persistence of *Brucella abortus* in mice. *Infect Immun* **68**, 4102–4107.

Höppner, C., Liu, Z., Domke, N., Binns, A. N. & Baron, C. (2004). VirB1 orthologs from *Brucella suis* and pKM101 complement defects of the lytic transglycosylase required for efficient type IV secretion from *Agrobacterium tumefaciens*. *J Bacteriol* **186**, 1415–1422.

Hwang, H. H. & Gelvin, S. B. (2004). Plant proteins that interact with VirB2, the *Agrobacterium tumefaciens* pilin protein, mediate plant transformation. *Plant Cell* **16**, 3148–3167.

Jones, A. L., Shirasu, K. & Kado, C. I. (1994). The product of the *virB4* gene of *Agrobacterium tumefaciens* promotes accumulation of VirB3 protein. *J Bacteriol* **176**, 5255–5261.

Knoblauch, N. T., Rudiger, S., Schonfeld, H. J., Driessen, A. J., Schneider-Mergener, J. & Bukau, B. (1999). Substrate specificity of the SecB chaperone. *J Biol Chem* **274**, 34219–34225.

Koraimann, G. (2003). Cell wall degrading enzymes in macromolecular transport systems of Gram-negative bacteria. *Cell Mol Life Sci* **60**, 2371–2388.

Kromayer, M., Wilting, R., Tormay, P. & Böck, A. (1996). Domain structure of the prokaryotic selenocysteine-specific elongation factor SelB. *J Mol Biol* **262**, 413–420.

Kumar, R. B. & Das, A. (2001). Functional analysis of the *Agrobacterium tumefaciens* T-DNA transport pore protein VirB8. *J Bacteriol* **183**, 3636–3641.

Kumar, R. B. & Das, A. (2002). Polar location and functional domains of the *Agrobacterium tumefaciens* DNA transfer protein VirD4. *Mol Microbiol* **43**, 1523–1532.

Laemmli, U. K. (1970). Cleavage of structural proteins during the assembly of the head of bacteriophage T4. *Nature* **227**, 680–685.

Lehnherr, H., Hansen, A.-M. & Ilyina, T. (1998). Penetration of the bacterial cell wall: a family of lytic transglycosylases in bacteriophages and conjugative plasmids. *Mol Microbiol* **30**, 454–457.

Leung, A. K., Duewel, H. S., Honek, J. F. & Berghuis, A. M. (2001). Crystal structure of the lytic transglycosylase from bacteriophage lambda in complex with hexa-*N*-acetylchitohexaose. *Biochemistry* **40**, 5665–5673.

Liu, J. & Rost, B. (2003). NORSp: predictions of long regions without regular secondary structure. *Nucleic Acids Res* **31**, 3833–3835.

Livingstone, C. D. & Barton, G. J. (1993). Protein sequence alignments: a strategy for the hierarchical analysis of residue conservation. *Comput Appl Biosci* **9**, 745–756.

Llanos, R., Chevrier, V., Ronjat, M. & 7 other authors (1999). Tubulin binding sites on gamma-tubulin: identification and molecular characterization. *Biochemistry* **38**, 15712–15720.

Llosa, M. & O'Callaghan, D. (2004). Euroconference on the Biology of Type IV Secretion Processes: bacterial gates into the outer world. *Mol Microbiol* **53**, 1–8.

Llosa, M., Zupan, J., Baron, C. & Zambryski, P. C. (2000). The N- and C-terminal portions of the *Agrobacterium* VirB1 protein independently enhance tumorgenesis. *J Bacteriol* **182**, 3437–3445.

Lutzmann, M., Kunze, R., Buerer, A., Aebi, U. & Hurt, E. (2002). Modular self-assembly of a Y-shaped multiprotein complex from seven nucleoporins. *EMBO J* **21**, 387–397.

Maniatis, T. A., Fritsch, E. F. & Sambrook, J. (1982). *Molecular Cloning: a Laboratory Manual*. Cold Spring Harbor, NY: Cold Spring Harbor Laboratory.

Middleton, R., Sjölander, K., Krishnamurthy, N., Foley, J. & Zambryski, P. (2005). Predicted hexameric structure of the *Agrobacterium* VirB4 C terminus suggests VirB4 acts as a docking site during type IV secretion. *Proc Natl Acad Sci U S A* **102**, 1685–1690.

Mushegian, A. R., Fullner, K. J., Koonin, E. V. & Nester, E. W. (1996). A family of lysozyme-like virulence factors in bacterial pathogens. *Proc Natl Acad Sci U S A* **93**, 7321–7326.

Needleman, S. B. & Wunsch, C. D. (1970). A general method applicable to the search for similarities in the amino acid sequence of two proteins. *J Mol Biol* **48**, 443–453.

O'Callaghan, D., Cazevieille, C., Allardet-Servent, A., Boschiroli, M. L., Bourg, G., Foulongne, V., Frutos, P., Kulakov, Y. & Ramuz, M. (1999). A homologue of the *Agrobacterium tumefaciens* VirB and *Bordetella pertussis* Ptl type IV secretion systems is essential for intracellular survival of *Brucella suis*. *Mol Microbiol* **33**, 1210–1220.

Odenbreit, S., Gebert, B., Püls, J., Fischer, W. & Haas, R. (2001). Interaction of *Helicobacter pylori* with professional phagocytes: role of the *cag* pathogenicity island and translocation, phosphorylation and processing of CagA. *Cell Microbiol* **3**, 21–31.

Reimer, U., Reineke, U. & Schneider-Mergener, J. (2002). Peptide arrays: from macro to micro. *Curr Opin Biotechnol* **13**, 315–320.

Reineke, U., Kramer, A. & Schneider-Mergener, J. (1999). Antigen sequence- and library-based mapping of linear and discontinuous protein-protein-interaction sites by spot synthesis. *Curr Top Microbiol Immunol* **243**, 23–36.

Rohde, M., Püls, J., Buhrdorf, R., Fischer, W. & Haas, R. (2003). A novel sheathed surface organelle of the *Helicobacter pylori* type IV secretion system. *Mol Microbiol* **49**, 219–234.

Rost, B. (1996). PHD: predicting one-dimensional protein structure by profile-based neural networks. *Methods Enzymol* **266**, 525–539.

Schmidt-Eisenlohr, H., Domke, N., Angerer, C., Wanner, G., Zambryski, P. C. & Baron, C. (1999). Vir proteins stabilize VirB5 and mediate its association with the T pilus of *Agrobacterium tumefaciens*. *J Bacteriol* **181**, 7485–7492.

Shamaei-Tousi, A., Cahill, R. & Frankel, G. (2004). Interaction between protein subunits of the type IV secretion system of *Bartonella henselae*. *J Bacteriol* **186**, 4796–4801.

Sieira, R., Comerci, D. J., Sanchez, D. O. & Ugalde, R. A. (2000). A homologue of an operon required for DNA transfer in *Agrobacterium* is required in *Brucella abortus* for virulence and intracellular multiplication. *J Bacteriol* **182**, 4849–4855.

Smith, T. F. & Waterman, M. S. (1981). Overlapping genes and information theory. *J Theor Biol* **91**, 379–380.

Thunnissen, A. M., Dijkstra, A. J., Kalk, K. H., Rozeboom, H. J., Engel, H., Keck, W. & Dijkstra, B. W. (1994). Doughnut-shaped structure of a bacterial muramidase revealed by X-ray crystallography. *Nature* **367**, 750–753.

van Asselt, E. J., Dijkstra, A. J., Kalk, K. H., Takacs, B., Keck, W. & Dijkstra, B. W. (1999). Crystal structure of *Escherichia coli* lytic transglycosylase Slt35 reveals a lysozyme-like catalytic domain with an EF-hand. *Structure Fold Des* **7**, 1167–1180.

van Asselt, E. J., Kalk, K. H. & Dijkstra, B. W. (2000). Crystallographic studies of the interactions of *Escherichia coli* lytic transglycosylase Slt35 with peptidoglycan. *Biochem* **39**, 1924–1934.

Ward, D., Draper, O., Zupan, J. R. & Zambryski, P. C. (2002). Peptide linkage mapping of the *A. tumefaciens vir*-encoded type IV secretion system reveals novel protein subassemblies. *Proc Natl Acad Sci U S A* **99**, 11493–11500.

Winans, S. C. & Walker, G. C. (1985). Conjugal transfer system of the N incompatibility plasmid pKM101. *J Bacteriol* **161**, 402–410.

Yanisch-Perron, C., Vieira, J. & Messing, J. (1985). Improved M13 phage cloning vectors and host strains: nucleotide sequence of the M13mp18 and pUC18 vectors. *Gene* **33**, 103–119.

Yeo, H.-J. & Waksman, G. (2004). Unveiling molecular scaffolds of the type IV secretion system. *J Bacteriol* **186**, 1919–1926.

Yeo, H.-J., Yuan, Q., Beck, M. R., Baron, C. & Waksman, G. (2003). Structural and functional characterization of the VirB5 protein from the type IV secretion system encoded by the conjugative plasmid pKM101. *Proc Natl Acad Sci U S A* **100**, 15947–15962.

Yuan, Q., Carle, A., Gao, C., Sivanesan, D., Aly, K., Höppner, C., Krall, L., Domke, N. & Baron, C. (2005). Identification of the VirB4-VirB8-VirB5-VirB2 pilus assembly sequence of type IV secretion systems. *J Biol Chem* **280**, 26349–26359.

Zahrl, D., Wagner, M., Bischof, K., Bayer, M., Zavecz, B., Beranek, A., Ruckenstuhl, C., Zarfel, G. E. & Koraimann, G. (2005). Peptidoglycan degradation by specialized lytic transglycosylases associated with type III and type IV secretion systems. *Microbiology* **151**, 3455–3467.

Zupan, J., Muth, T. R., Draper, O. & Zambryski, P. C. (2000). The transfer of DNA from *Agrobacterium tumefaciens* into plants: a feast of fundamental insights. *Plant J* **23**, 11–28.